

## Electronic structures of double perovskites $\text{Sr}_2(\text{Mn}_{1-x}\text{Fe}_x)\text{MoO}_6$ : LSDA + $U$ studies

This article has been downloaded from IOPscience. Please scroll down to see the full text article.

2005 J. Phys.: Condens. Matter 17 2035

(<http://iopscience.iop.org/0953-8984/17/12/024>)

View [the table of contents for this issue](#), or go to the [journal homepage](#) for more

Download details:

IP Address: 129.252.86.83

The article was downloaded on 27/05/2010 at 20:33

Please note that [terms and conditions apply](#).

# Electronic structures of double perovskites $\text{Sr}_2(\text{Mn}_{1-x}\text{Fe}_x)\text{MoO}_6$ : LSDA + $U$ studies

Zhongqin Yang<sup>1</sup> and Ling Ye

Surface Physics Laboratory (National Key Laboratory), Fudan University, Shanghai 200433, People's Republic of China

E-mail: zyang@fudan.edu.cn

Received 29 October 2004, in final form 12 January 2005

Published 11 March 2005

Online at [stacks.iop.org/JPhysCM/17/2035](http://stacks.iop.org/JPhysCM/17/2035)

## Abstract

Electronic structures of double perovskites  $\text{Sr}_2(\text{Mn}_{1-x}\text{Fe}_x)\text{MoO}_6$  ( $x = 0.0, 0.5, 1.0$ ) have been studied by using the LSDA +  $U$  method, where the on-site Coulomb interaction  $U$  of localized d electrons has been considered in the local-spin density approximation. The band structure of  $\text{Sr}_2\text{MnMoO}_6$  with antiferromagnetic structure is found to be semiconducting with a gap of 0.5 eV, which is in good agreement with recent optical absorption results. The optical absorption corresponding to this optical threshold is found to be a non-vertical transition, which can occur only if a non-zero momentum such as from phonons participates in the transition. With the increase of  $x$ , the band becomes half-metallic and ferrimagnetic. These semiconductor–metal and magnetic structure transitions can be rationalized by different characteristics of charge transfers between Fe–Mo and Mn–Mo via intermediate O 2p orbitals. The down-spin Mo  $t_{2g}$  states cross the Fermi energy ( $E_F$ ) in the presence of Fe ions. With the increase of  $x$ , more states cross over  $E_F$ , which explains the high conductivity in the compound with large  $x$  observed in experiment.

In recent years we have witnessed an increased interest in the study of transition-metal oxides with ordered double-perovskite structures,  $\text{A}_2\text{BB}'\text{O}_6$  ( $\text{A} = \text{Sr}, \text{Ca}, \text{Ba}, \text{La}, \text{etc}$ ;  $\text{B}, \text{B}'$  are heterovalent transition metals, such as  $\text{B} = \text{Fe}, \text{Cr}, \text{Mn}, \dots$ ;  $\text{B}' = \text{Mo}, \text{Re}, \text{W}, \dots$ ). Novel and attractive properties that can be useful in future spintronic device applications have been demonstrated, such as the large tunnelling-type magnetoresistance observed at room temperature [1, 2] and the evident low field magnetoresistance [3] found in FeMo double perovskites. These features have been ascribed to highly spin-polarized nature and/or high-magnetic Curie temperature  $T_C$  (350–450 K for  $\text{A}_2\text{FeMoO}_6$ ,  $\text{A} = \text{Ca}, \text{Sr}, \text{and Ba}$  [4, 5]). In FeMo metallic compounds, Fe ions ( $\text{Fe}^{3+}, 3d^5$ ) are in the high spin state of  $S = 5/2$  according

<sup>1</sup> Author to whom any correspondence should be addressed.

to Hund's rule, while  $\text{Mo}^{5+}(4d^1)$  are highly ionized with valence spin states of  $S = 1/2$ . A large antiferromagnetic superexchange (SE) interaction between  $\text{Fe}^{3+}$  and  $\text{Mo}^{5+}$  induces a ferrimagnetic and half-metallic (completely spin-polarized states with semiconducting spin-up and metallic spin-down bands) structure [1].

By varying different cations or doping with other alkaline ions at A sites, like the formula of  $(AA')_2BB'O_6$  ( $BB' = \text{FeMo}$  or  $\text{FeRe}$ , etc), very rich electronic and magnetic properties can be obtained [3, 6–9]. For example, in the compounds with  $AA' = \text{BaBa}$ ,  $\text{BaSr}$ , ... or  $\text{CaCa}$ ,  $BB' = \text{FeRe}$ , the Curie temperature is found to increase anomalously from 303 K for  $\text{BaBa}$  ( $\text{Ba}_2$ ) to 522 K for  $\text{Ca}_2$ , which has been rationalized by large lattice distortion from cubic to monoclinic due to different cation sizes of Ba and Ca ions [7]. The electronic states transfer correspondingly from metallic behaviour with not too large coercivity in the cubic system to semiconducting behaviour with huge coercivity in the monoclinic structure. The electronic structures of the compounds with doping on B sites, however, have seldom been investigated up to now. There can be two different SE interactions simultaneously occurring in such a kind of doped compounds, which have only been investigated by Jung *et al* [10], to our knowledge. By optical measurement, they studied the electronic structures of  $\text{FeMo}$  double perovskites with doping of Mn at Fe sites in the structure  $\text{Sr}_2(\text{Mn}_{1-x}\text{Fe}_x)\text{MoO}_6$ . The compounds are appropriate candidates for the investigation of the semiconductor–metal transition since the two end members are antiferromagnetic (AFM) semiconductor and ferrimagnetic (FiM) half metallic for  $x = 0$  and 1, respectively. The obtained optical conductivity spectra, however, cannot be interpreted quantitatively by them due to the lack of available band structures [10].

In this work, we study theoretically the electronic states of  $\text{Sr}_2(\text{Mn}_{1-x}\text{Fe}_x)\text{MoO}_6$  ( $x = 0.0, 0.5, 1.0$ ) by the LSDA +  $U$  method. The obtained electronic structures explain well the experimentally observed optical conductivity spectra [10], especially the optical threshold. The band structures also illustrate reasonably the semiconductor–metal and AFM–FiM transitions with the increase of  $x$ . The transitions can be ascribed to different characters of charge transfer between Fe–Mo and Mn–Mo via intermediate O 2p states with the variation of  $x$ . Obvious spin polarization appears in the  $t_{2g}$  states of Mo ions neighbouring Fe ions, but not for the ions neighbouring Mn ions. The down-spin Mo  $t_{2g}$  states begin to cross the Fermi level  $E_F$  in the presence of Fe. With the increase of the Fe component, the compounds have high conductivity.

The experimentally observed crystalline structures from [11] are adopted in the calculation for the two ends,  $\text{Sr}_2(\text{Mn}, \text{Fe})\text{MoO}_6$ . They both have cubic structures, with  $Fm\bar{3}m$  (No 225) symmetry<sup>2</sup>. The geometric structure of  $\text{Sr}_2\text{MnMoO}_6$  is given in the upper inset of figure 1. In the structure, both Mn and Mo atoms form a face-centred cubic (fcc) lattice with the displacement of half of the lattice constant. Oxygen atoms are located near the centre of each nearest-neighbouring Mn–Mo pair [11]. (To simplify the figure, only the six oxygen atoms around the centre Mn ion are shown.) The arrows on Mn atoms in the figure indicate the spin directions, which form an AFM arrangement of Mn ions according to experimental reports [12]<sup>3</sup>. Due to the AFM arrangement of Mn ions in  $\text{Sr}_2\text{MnMoO}_6$ , the symmetry of the structure is lowered from  $Fm\bar{3}m$  to  $P4/mmm$  (No 123). The unit cell is given by a dotted curve in the inset. For  $\text{Sr}_2\text{FeMoO}_6$ , the Fe and Mo magnetic ions form an FiM structure, whose unit cell, shown by thin lines in the inset, is half of that of  $\text{Sr}_2\text{MnMoO}_6$ . The structure of the doping compound,  $\text{Sr}_2\text{Mn}_{0.5}\text{Fe}_{0.5}\text{MoO}_6$ , is also a cubic one with the lattice constant derived from the interpolation of those of the two end members since no experimental result

<sup>2</sup> Although monoclinic structure is reported for  $\text{Sr}_2\text{MnMoO}_6$  in [21], the distortion from the monoclinic structure to the cubic one is very small. The effects from the distortion on the band structure should be negligible.

<sup>3</sup> Since there are in total four kinds of AFM arrangements in fcc structure and no experimental report on the detailed magnetic structures in the compound, the simplest type-I AFM structure was chosen in the calculation as shown in the upper inset of figure 1.

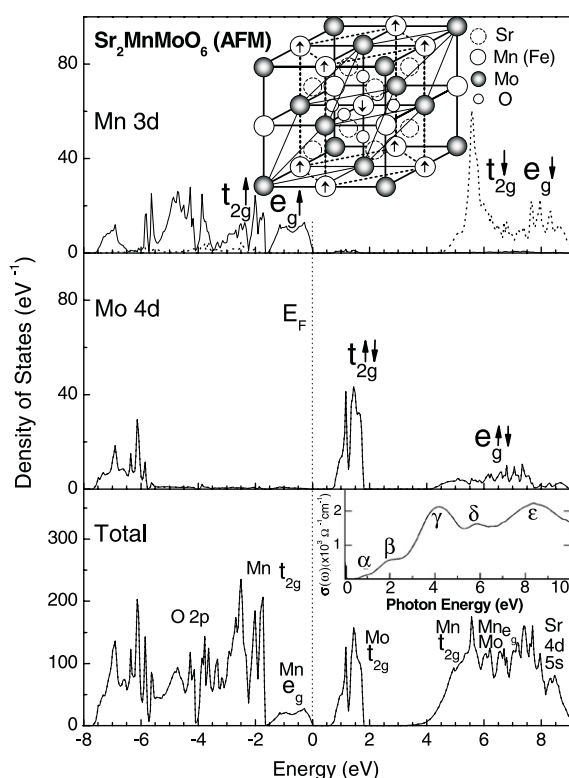


**Figure 1.** The total and partial densities of states of Mn and Mo ions in  $\text{Sr}_2\text{MnMoO}_6$  obtained by using the LSDA +  $U$  method. The solid and dotted curves represent spin-up and down bands, respectively. The energy zero is set at the Fermi level. The upper inset gives a sketch of the cubic double-perovskite structure of  $\text{Sr}_2\text{MnMoO}_6$  with AFM phase, whose unit cell is given by dotted curves. The arrows at Mn atoms indicate the spin directions. The lower inset shows the experimental optical conductivity spectrum from [10].

is available. The cations Mn and Fe in the doping compound occupy alternately the Mn sites in  $\text{Sr}_2\text{MnMoO}_6$ . The sketch of the unit cell of the doped compound can also be expressed by the dotted lines in the inset of figure 1, but with one Fe atom occupying one of the two original Mn positions.

The first-principle band structure calculations were performed by using the linear muffin-tin orbital (LMTO) method [13] with the atomic-sphere approximation, based on LSDA +  $U$  schemes [14, 15], where the on-site Coulomb interaction  $U$  correction was taken into account to improve the results of a system containing d electrons [16]. The details of the scheme of considering  $U$  interaction can be found in [17]. The Hartree potential is expanded in terms of spherical harmonics up to  $L = 4$ , and an exchange–correlation potential of von Barth–Hedin type [18] is adopted. Sr 5s4p4d, Mn(Fe) 4s4p3d, Mo 5s5p4d, and O 2s2p orbitals were taken as the basis set in the calculation. The radii of the muffin-tin spheres chosen for the atoms (in atomic units) are Sr 3.8, Fe 2.3, Mn 2.5, Mo 2.1, and O 1.5, respectively. It has been verified that the structures are close enough that no empty sphere is needed to insert in the unit cells. It is found that all the states, except for Sr 5s4d, Mn(Fe)3d, Mo 4d, and O 2p, are located far away from  $E_F$ . They are not included in the following analysis due to little effect on the results one is interested in. The averaged Coulomb  $U$  parameters taken for Mn and Fe ions are 3.0 and 4.0 eV, respectively. The exchange  $J$  parameters for them are approximately taken as 0.7 eV. The  $U$  and  $J$  parameters used for the weakly correlated Mo 4d are 1.0 and 0.2 eV [19], respectively.

For  $\text{Sr}_2\text{MnMoO}_6$ , two different magnetic structures, AFM [12] and paramagnetic (PM) [11], have been reported experimentally. It has been unclear until now which state is the ground one [20]. The total energies of the two structures are calculated in the present

work. The obtained total energy of the AFM structure is found to be much lower than that of PM by 952 meV/Mn, implying that the AFM structure is the ground state of the compound. The total and partial densities of states (DOSs) of Mn and Mo ions in  $\text{Sr}_2\text{MnMoO}_6$  with AFM phase are given in figure 1. The Mn 3d spin-up states are mainly located below  $E_F$ , while the spin-down ones are above  $E_F$ , indicating the near half-filling of Mn 3d bands ( $3d^5$ ). There is a peak of Mn 3d  $t_{2g}\downarrow$  states at the energy of 5.5 eV, while the Mn  $t_{2g}\uparrow$  are located in a broad energy region from  $-7.5$  to  $-1.5$  eV. It can be ascribed to the strong hybridization between Mn  $t_{2g}\uparrow$  and O 2p, which occupy almost the same energy region. The spin polarization of Mn 3d shown in the partial DOS is very strong with the spin splitting energy of about 8.0 eV [17]<sup>4</sup>. Sharply contrasting to Mn ions, the spin-up and down bands of Mo 4d overlap completely. This gives rise to non-magnetic Mo ions, in agreement with experiment [12]. From the DOS of Mo 4d, it is obvious that Mo  $t_{2g}\uparrow\downarrow$  and  $e_g\uparrow\downarrow$  are basically located above  $E_F$ , except for few states occupying the region below  $E_F$  due to the hybridization. This gives the formal valence configuration on Mo ions of  $4d^0$ . Therefore, the antiferromagnetic interaction in the compound can be considered to originate from the long range SE interaction of Mn ions ( $\text{Mn}^{2+}$ , near half-filling) via the medial non-magnetic  $\text{MoO}_6^{0-}$  molecule.

The optical conductivity spectrum of  $\text{Sr}_2\text{MnMoO}_6$  measured by Jung *et al* [10] is given in the inset at the bottom of figure 1. There is an obvious optical gap about 0.5 eV shown in the spectrum, which can be rationalized by the gap with almost the same magnitude between Mn  $e_g$  and Mo  $t_{2g}$  bands (see the total DOS in figure 1). Since the compound is an indirect gap semiconductor (see the band structure in figure 4(a): the top of the valence band is at X, while the bottom of the conduction band is at the Z point in the first Brillouin zone), this non-vertical interband transition corresponding to the optical threshold (about 0.5 eV) can occur only if a non-zero momentum such as from phonons participates in the transition. The probability of such indirect transition is expected to be lower than that of a direct one. The absorption energy of the optical direct transition from the top of the valence band of Mn  $e_g$  at X is near 1.0 eV, which corresponds very well to the lowest peak  $\alpha$  in the experimental spectrum. The absorption peak  $\beta$  in the spectrum can be assigned to optical transitions from Mn ( $e_g, t_{2g}$ , below  $E_F$ ) to Mo  $t_{2g}$ . The optical transition from the high peak of O 2p (at about  $-2.5$  eV) to the lowest empty band Mo  $t_{2g}$  (at about 1.5 eV) illustrates well the  $\gamma$  peak at 4.0 eV in the optical conductivity spectrum. The assignment of the peaks ( $\delta$  and  $\varepsilon$ ) in the high energy region is very complex. They can be contributed by any of the transitions of O 2p  $\rightarrow$  (Mo, Mn)  $t_{2g}$  (above  $E_F$ ) and O 2p  $\rightarrow$  (Mn, Mo)  $e_g$  at the same transition energy. Optical transitions between some d–d states, such as Mn  $e_g$  (below  $E_F$ ) to Mn  $t_{2g}$  and (Mn, Mo)  $e_g$  (above  $E_F$ ) also possibly contribute to the two high energy peaks, although the intensities of these d–d transitions are generally lower than those of p–d.

The obtained bandgap and the local magnetic moments on Mn and Mo ions in the compound are given in table 1. The bandgap is in good agreement with the experimental result. The compound belongs to the Mott–Hubbard-type insulators [17] due to the gap formed by Mn  $e_g$  and Mo  $t_{2g}$  bands. The gap is opened directly by the on-site Coulomb interaction. It is found that the gap cannot be opened if Hubbard  $U$  interaction is not considered in the calculation. The magnetic moment on Mn ions in the compound is about  $4.7 \mu_B$  (close to its maximum  $5.0 \mu_B$ ). This is reasonable since the Mn 3d bands are found to be nearly half filled ( $3d^5$ ) in the present work. Moritomo *et al*, however, estimated the moment on Mn ions of  $5.74 \mu_B$ , which seems to be too large [11]. At the same time Muñoz *et al* proposed a possible non-collinear arrangement of magnetic moments in the compound [21]. This problem needs to be further investigated.

<sup>4</sup> The spin splitting energy is strongly dependent on the on-site Coulomb interaction. It increases sensitively with the  $U$  parameter, especially when the bands are half-filled (see [17]).

**Table 1.** Band structures and magnetic moments in  $\text{Sr}_2\text{Mn}_{1-x}\text{Fe}_x\text{MoO}_6$  ( $x = 0.0, 0.5, 1.0$ ) obtained by using LSDA +  $U$  approaches, compared with available related experimental results. 'M' represents a metallic band. 'HM' means 'half metallic'.

		Magnetic moment ( $\mu_B$ )				
$\text{Sr}_2\text{MnMoO}_6$ (AFM)	Gap (eV)	Mn	Mo			
This work	0.6	4.7	0.0			
Experimental	0.5 <sup>a</sup>	4.2 <sup>b</sup> , 5.74 <sup>c</sup>	0.0 <sup>b,c</sup>			
		Magnetic moment ( $\mu_B$ )				
$\text{Sr}_4\text{FeMnMo}_2\text{O}_{12}$ (FiM)	Band structure	Mn	Fe	Mo <sub>1</sub>	Mo <sub>2</sub>	Total
This work	M(HM)	4.7	4.1	0.0(2)	-0.3	9.0
Experimental	M <sup>a</sup>					
		Magnetic moment ( $\mu_B$ )				
$\text{Sr}_2\text{FeMoO}_6$ (FiM)	Band structure	Fe	Mo	Total		
This work	M(HM)	4.1	-0.5	4.0		
Experimental	M <sup>a,c,d</sup>	4.1 <sup>c</sup>	-0.5 <sup>c</sup>	3.6 <sup>d</sup> , 3.3 <sup>c</sup>		

<sup>a</sup> Reference [10].

<sup>b</sup> Reference [21].

<sup>c</sup> Reference [24].

<sup>d</sup> Reference [26].

The unusual half-metallic nature is found for  $\text{Sr}_2\text{FeMoO}_6$  with FiM structure in the calculation, as previous theoretical studies predicted [1, 22–24]. The interesting phenomenon in the compound is that Fe 3d bands are also near half-filling, similarly to the Mn 3d in  $\text{Sr}_2\text{MnMoO}_6$ . There is thus formally one electron occupying the Mo 4d band, being easily seen from the partial DOS of Mo 4d in figure 2. Both the half-filling of 3d states of Fe and Mn in the two different compounds can be due to the fact that half- or fully filled states are more stable than other configurations, according to Hund's rule. There is small, but evident, spin splitting occurring in the Mo 4d band in  $\text{Sr}_2\text{FeMoO}_6$ , in strong contrast to the non-magnetic Mo ions in  $\text{Sr}_2\text{MnMoO}_6$ . The obvious spin polarization of Mo 4d states causes only one of the spin states (spin down) crossing  $E_F$  to become possible. It leads to half-metallic nature of the compound (see the total DOS in figure 2). Since the directions of magnetic moments of Fe and Mo ions are up and down, respectively, it gives ferrimagnetic structure. Therefore, the SE interaction between the two ions (mediated by O 2p states) is negative in the compound. From the partial DOSs of Mn and Fe in the two compounds, it can be seen that Fe 3d states occupy a lower energy region than the corresponding Mn 3d. For example, Mn  $t_{2g}\downarrow$  is located near Mo  $e_g\uparrow\downarrow$  in energy, while Fe  $t_{2g}\downarrow$  is very close to Mo  $t_{2g}\uparrow\downarrow$ . This can explain why there is no corresponding peak ( $\delta$ ) observed in the optical conductivity spectrum at 6.0 eV in  $\text{Sr}_2\text{FeMoO}_6$  [10]. In table 1, the experimental total magnetic moment is essentially less than the theoretical value, which can be ascribed to antisite disorder at the Fe and Mo sites occurring in the experimental sample [3].

The partial and total DOSs of  $\text{Sr}_2\text{Mn}_{0.5}\text{Fe}_{0.5}\text{MoO}_6$  with FiM phase are shown in figure 3, where Mo<sub>1</sub> ions have four Mn and two Fe ions located nearest, while Mo<sub>2</sub> have four Fe and two Mn ions instead. It is very evident that Mn and Fe 3d states in this doped compound are still near half-filling. This gives rise to different valence states of Mo<sub>1</sub> and Mo<sub>2</sub> ions in the material (see the partial DOS of Mo<sub>1</sub> and Mo<sub>2</sub> in figure 3). Due to the strong hybridization between these magnetic ions, there are also few states across  $E_F$  for the spin-down Fe 3d and

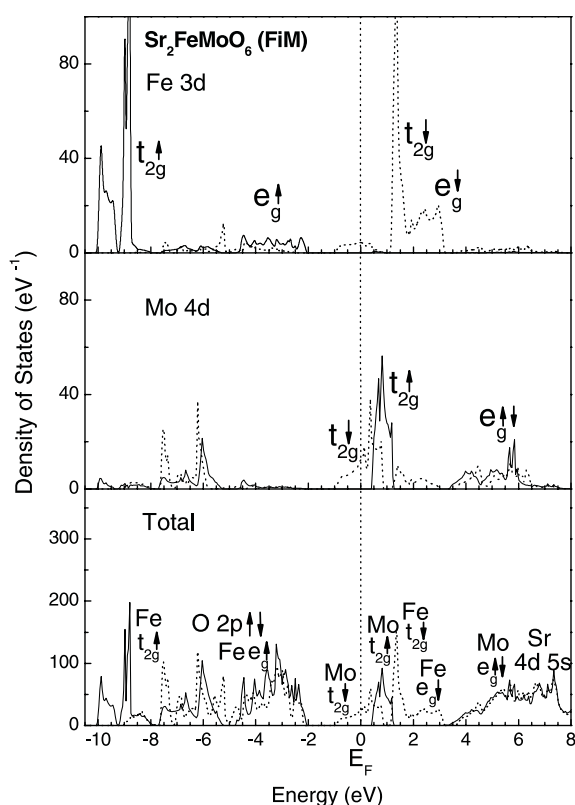


**Figure 2.** The total and partial densities of states of Fe and Mo ions in  $\text{Sr}_2\text{FeMoO}_6$  with FiM phase.

$\text{Mo}_1$  4d. The local magnetic moments obtained for these magnetic ions are given in table 1. The magnetic moments on Mn and Fe are the same as those in the end members, while the moments on  $\text{Mo}_2$  are a little less than in  $\text{Sr}_2\text{FeMoO}_6$  since there are two Mn ions around the ion besides four Fe ions. There is also a very small magnetic moment found on  $\text{Mo}_1$  ions. The spin-up bands of Mo 4d do not cross  $E_F$ , which leads to half-metallic bands in the compound, as in  $\text{Sr}_2\text{FeMoO}_6$ . Since Mn  $e_g \uparrow$  bands are very close to  $E_F$ , the bandgap of the spin-up band in this doped compound is much smaller than that in  $\text{Sr}_2\text{FeMoO}_6$ . Compared to the semiconducting  $\text{Sr}_2\text{MnMoO}_6$  with AFM structure, the metallic phase in FiM  $\text{Sr}_2\text{Mn}_{0.5}\text{Fe}_{0.5}\text{MoO}_6$  is found to be caused by two different SE interactions between Mn–O– $\text{Mo}_1$  and Fe–O– $\text{Mo}_2$ . The different features of charge transfer between Fe/Mn 3d states and Mo 4d states cause the valence bands of one of the Mo ions crossing  $E_F$  in the presence of Fe in the compound. This characteristic of the semiconductor–metal transition is very different from that found in  $\text{Sr}_2\text{FeMo}_{1-x}\text{W}_x\text{O}_6$ , which has been interpreted in terms of a valence fluctuation between  $\text{Fe}^{2+}/(\text{W}, \text{Mo})^{6+}$  and  $\text{Fe}^{3+}/(\text{W}, \text{Mo})^{5+}$  [25]. The magnetic moments of Fe and Mn ions in figure 3 are in the same direction. They are opposite to those of two Mo ions. We also calculated another kind of ferrimagnetic structure in the compound, where the magnetic moment on Mn ions is opposite to that the in above case. The magnitudes of all the moments are hardly changed. The total energy of this alternative magnetic phase is found to be higher than that of the previous structure by only 53 meV per unit cell. Such a low energy difference between the two magnetic structures means that it is not difficult to flip the spin direction on Mn ions in the compound.

The band structure varying with the doping level  $x$  ( $x = 0.0, 0.5, 1.0$ ) in  $\text{Sr}_2\text{Mn}_{1-x}\text{Fe}_x\text{MoO}_6$  can be seen clearly in figure 4. There is an obvious gap formed by

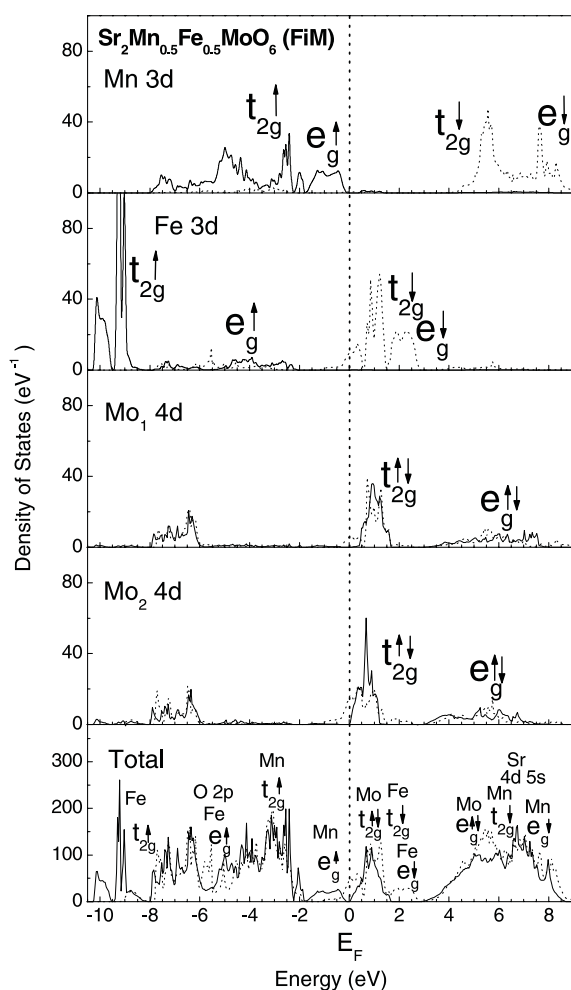


**Figure 3.** The total and partial densities of states of magnetic ions in  $\text{Sr}_2\text{Mn}_{0.5}\text{Fe}_{0.5}\text{MoO}_6$  with FiM phase.

Mn  $e_g$  and Mo  $t_{2g}$  states in  $\text{Sr}_2\text{MnMoO}_6$ . After doping with the Fe component, the spin-up and down bands of Mo  $t_{2g}$  states split. The spin-down ones move down in the energy spectrum and cross  $E_F$ . With the increase of the Fe component, more Mo  $t_{2g\downarrow}$  states cross over  $E_F$  (as seen from figure 4(c))<sup>5</sup>. By integrating the spin-down total DOS from  $-1$  eV to  $E_F$ , nearly 0.5 electron-type carrier per Mo atom is obtained in  $\text{Sr}_2\text{Mn}_{0.5}\text{Fe}_{0.5}\text{MoO}_6$ , while nearly 1.0 carrier is obtained for  $\text{Sr}_2\text{FeMoO}_6$  (corresponding to the density of the conduction electrons of  $1.1 \times 10^{22} \text{ cm}^{-3}$ , consistent with the experimental measured value [4]). From figures 4(b) and (c), it is also found that the bands of Mo  $t_{2g\downarrow}$  in  $\text{Sr}_2\text{Mn}_{1-x}\text{Fe}_x\text{MoO}_6$  are flatter than those in  $\text{Sr}_2\text{FeMoO}_6$ , indicating that the states in the former are more localized than those in the latter. These behaviours could explain why the resistivity of  $\text{Sr}_2\text{Mn}_{0.5}\text{Fe}_{0.5}\text{MoO}_6$  is much larger than that of  $\text{Sr}_2\text{FeMoO}_6$  observed in experiment [10]. From the trend of the band structure varying with the doping level  $x$ , it can be predicted that the resistivity of the compound increases with the decrease of  $x$ . The compound transfers to a semiconductor when  $x = 0$ , namely the end member of  $\text{Sr}_2\text{MnMoO}_6$ . This variation characteristic of the resistivity in the compounds can

<sup>5</sup> The bands of  $\text{Sr}_2\text{Mn}_{0.5}\text{Fe}_{0.5}\text{MoO}_6$  are much denser than those of  $\text{Sr}_2\text{FeMoO}_6$  in figure 4 because the first Brillouin zone of the former is half of that of the latter and the bands in the second Brillouin zone are folded into the first one.



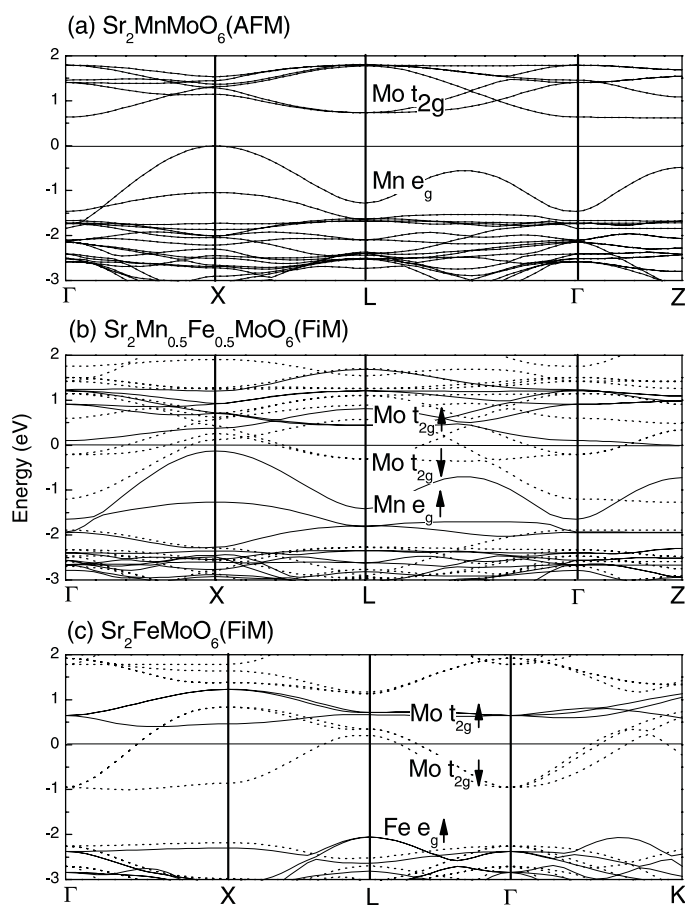


**Figure 4.** The band structures near  $E_F$  of (a)  $\text{Sr}_2\text{MnMoO}_6$ , (b)  $\text{Sr}_2\text{Mn}_{0.5}\text{Fe}_{0.5}\text{MoO}_6$ , and (c)  $\text{Sr}_2\text{FeMoO}_6$ .

be ascribed to the decrease/increase of the Fe/Mn component as well as the magnetic structures varying from FiM to AFM in the process.

Since electronic structures of compounds containing d electrons are sensitive to the strength of on-site  $U$  interaction [17], it is of great importance to choose appropriate values of  $U$  parameters. For double perovskites  $\text{Sr}_2\text{FeMoO}_6$ , very different  $U$  values for Fe ions have been chosen by different researchers, such as 2.0 eV in [24], and 4.5 eV in [23]. To explore the effects of the on-site Coulomb energy on the band structure and the magnetic moment, we study the variation of the electronic structures of  $\text{Sr}_2\text{MnMoO}_6$  and  $\text{Sr}_2\text{FeMoO}_6$  with different strengths of the on-site  $U$  interaction. Figures 5(a) and (b) give the variation of the gap and the local magnetic moment at Mn ions with  $U_{\text{Mn}}$  parameter in  $\text{Sr}_2\text{MnMoO}_6$ , respectively. The gap in figure 5(a) increases sensitively and linearly with  $U_{\text{Mn}}$ . From previous analysis, the gap in  $\text{Sr}_2\text{MnMoO}_6$  is formed by bands of Mn  $e_g$  and Mo  $t_{2g}$ . The empty bands Mo  $t_{2g}\uparrow\downarrow$  are found not to change much with the variation of the on-site Coulomb interaction, while the occupied bands Mn  $e_g$  shift linearly to the lower energy region with  $U$ . This feature causes the gap to increase linearly with  $U$ . The magnetic moment on Mn ions also increases with the  $U$  interaction due to the strong spin polarization with large value of  $U$  [17]. The magnetic moment, however, would not exceed the maximum of  $5.0 \mu_B$  of  $\text{Mn}^{2+}$  ions (see figure 5(b)).

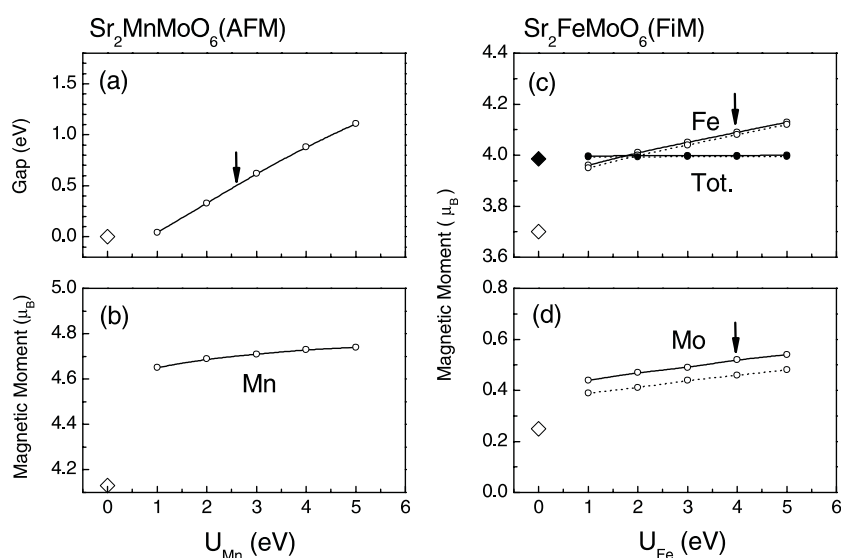


**Figure 5.** The variations of (a) energy gap and (b) magnetic moment at Mn ions in  $\text{Sr}_2\text{MnMoO}_6$  with  $U$  interaction on Mn ions; and the variations of magnetic moments of (c) Fe (open circles) and total (solid circles, per unit cell) and (d) Mo in  $\text{Sr}_2\text{FeMoO}_6$  with  $U$  interaction on Fe ions. The circles on solid and dotted lines represent the values obtained with and without considering the Hubbard interaction on Mo. The ‘diamond’ symbols in the figures represent the results obtained with the standard LSDA method. The ‘arrows’ show the positions corresponding to experimental results.

Figures 5(c) and (d) give the variation of Fe, total (per unit cell) and Mo magnetic moments in  $\text{Sr}_2\text{FeMoO}_6$  with the increase of  $U_{\text{Fe}}$ , respectively. The spin direction of magnetic moment of Mo ions, opposite to that of Fe ions, is not shown in the figure. In the two figures, the circles on solid and dotted lines represent the values obtained with and without considering the on-site  $U$  interaction on Mo ions, respectively. In figure 5(c), the Fe magnetic moment increases linearly with  $U_{\text{Fe}}$ , similarly to that in  $\text{Sr}_2\text{MnMoO}_6$ . The very interesting property in the compound is that the magnetic moment at Mo ions also increases linearly with  $U_{\text{Fe}}$ , although the rate of increase is not as fast as that of Fe ions. At the same time, compared with the results on the dotted and solid lines, it is found that the Mo magnetic moment is improved much when the on-site Coulomb interaction is considered for Mo ions, while the Fe magnetic moment increases only little in figure 5(c). Therefore, it can be concluded that the magnetic moment at the Mo site must not be intrinsic, but actually induced by the Fe magnetic moment through the hybridization between the Fe 3d–O 2p–Mo 4d states in the compound. In this sense, it is ferromagnetic structure that is obtained in the present work for  $\text{Sr}_2\text{FeMoO}_6$ , which directly confirms the conclusion in [24]. Due to the unusual half-metallic band structure in the compound, the total magnetic moment per unit cell in figure 5(c) keeps the integer value of  $4 \mu_B$ . The ‘diamond’ symbols in figure 5 give the results obtained without considering the on-site  $U$  interactions. It is found that both the gap and the local magnetic moments on magnetic ions are improved much by considering the  $U$  interactions. The  $U$  values corresponding to the experimental results of the gap for  $\text{Sr}_2\text{MnMoO}_6$  and the local magnetic moments of Fe and Mo ions in  $\text{Sr}_2\text{FeMoO}_6$ , listed in table 1, are about 2.6 and 4.0 eV for the two compounds, respectively. They are indicated by the ‘arrow’ symbols in the figures. Compared with the  $U$  values in standard perovskite, 5.5 eV ( $\text{LaMnO}_3$ ) and 6.0 eV ( $\text{LaFeO}_3$ ) [17], it can possibly be concluded that the on-site Coulomb interactions of 3d states of transition-metal ions in

double perovskites are weaker than those in standard perovskites. This must be due to the screening effect of Mo 4d states, which shows itinerant property to a certain extent, in the double perovskites [19].

In summary, we have investigated the electronic structures of double perovskites  $\text{Sr}_2(\text{Mn}_{1-x}\text{Fe}_x)\text{MoO}_6$  ( $x = 0.0, 0.5, 1.0$ ) using the LSDA +  $U$  method. The experimental observed optical conductivity spectrum of the compounds can be interpreted by the electronic structures obtained. Obvious spin polarization begins to appear in Mo  $t_{2g}$  states at the presence of Fe ions in the doped compounds. The down-spin Mo  $t_{2g}$  states cross the Fermi energy level, causing the compound to turn from an antiferromagnetic insulator into a ferrimagnetic half-metallic structure. From the calculation, the conductivity of the compounds is found to be relatively high with the increase of Fe component, in agreement with experimental results.

### Acknowledgment

The authors acknowledge support from NSF grant No 10304002 of China.

### References

- [1] Kobayashi K-I, Kimura T, Sawada H, Terakura K and Tokura Y 1998 *Nature* **395** 677
- [2] Kobayashi K-I, Kimura T, Tomioka Y, Sawada H, Terakura K and Tokura Y 1999 *Phys. Rev. B* **59** 11159
- [3] García-Hernández M, Martínez J L, Martínez-Lope M J, Casais M T and Alonso J A 2001 *Phys. Rev. Lett.* **86** 2443
- [4] Tomioka Y, Okuda T, Okimoto Y, Kumai R, Kobayashi K I and Tokura Y 2000 *Phys. Rev. B* **61** 422
- [5] Nakagawa T 1968 *J. Phys. Soc. Japan* **24** 806
- [6] Kato H, Okuda T, Okimoto Y, Tomioka Y, Oikawa K, Kamiyama T and Tokura Y 2004 *Phys. Rev. B* **69** 184412
- [7] De Teresa J M, Serrate D, Blasco J, Ibarra M R and Morellon L 2004 *Phys. Rev. B* **69** 144401
- [8] Frontera C, Rubi D, Navarro J, García-Muñoz J L and Fontcuberta J 2003 *Phys. Rev. B* **68** 012412
- [9] Willem J, Bos G and Attfield J P 2004 *Phys. Rev. B* **69** 094434
- [10] Jung J H, Oh S J, Kim M W, Noh T W, Kim J Y, Park J H, Lin H J, Chen C T and Moritomo Y 2002 *Phys. Rev. B* **66** 104415
- [11] Moritomo Y, Xu Sh, Machida A, Akimoto T, Nishibori E, Takata M and Sakata M 2000 *Phys. Rev. B* **61** R7827
- [12] Itoh M, Ohta I and Inaguma Y 1996 *Mater. Sci. Eng. B* **41** 55
- [13] Andersen O K 1975 *Phys. Rev. B* **12** 3060  
Andersen O K, Pawłowska Z and Jepsen O 1986 *Phys. Rev. B* **34** 5253  
Skriver H L 1984 *The LMTO Method* (Berlin: Springer)
- [14] Anisimov V I, Zaanen J and Andersen O K 1991 *Phys. Rev. B* **44** 943
- [15] Savrasov S Y 1996 *Phys. Rev. B* **54** 16470
- [16] Korotin M A, Ezhov S Yu, Solovyev I V and Anisimov V I 1996 *Phys. Rev. B* **54** 5309  
Sarma D D, Shanthi N, Barman S R, Hamada N, Sawada H and Terakura K 1995 *Phys. Rev. Lett.* **75** 1126
- [17] Yang Z, Huang Z, Ye L and Xie X 1999 *Phys. Rev. B* **60** 15674
- [18] von Barth U and Hedin L 1972 *J. Phys. C: Solid State Phys.* **5** 1629
- [19] Sarma D D, Mahadevan P, Saha-Dasgupta T, Ray S and Kumar A 2000 *Phys. Rev. Lett.* **85** 2549
- [20] Poddar A and Das S 2004 *Physica B* **344** 325
- [21] Muñoz A, Alonso J A, Casais M T, Martínez-Lope M J and Fernández-Díaz M T 2002 *J. Phys.: Condens. Matter* **14** 8817
- [22] Jeng H T and Guo C Y 2003 *Phys. Rev. B* **67** 094438
- [23] Wu H 2001 *Phys. Rev. B* **64** 125126
- [24] Moritomo Y, Xu Sh, Akimoto T, Machida A, Hamada N, Ohoyama K, Nishibori E, Takata M and Sakata M 2000 *Phys. Rev. B* **62** 14224
- [25] Ray S, Kumar A, Majumdar S, Sampathkumaran E V and Sarma D D 2000 *J. Phys.: Condens. Matter* **13** 607
- [26] Kim T H, Uehara M, Cheong S-W and Lee S 1999 *Appl. Phys. Lett.* **74** 1737